

revvity

# *In Vivo* Imaging Technologies in Basic and Preclinical Research

dr. Simon Koren

15.06.2023

omegac



## Ekipa v Sloveniji

Ana Rant

Aleš Hieng

dr. Andrej Hanzlowsky

dr. Anja Veronovski

dr. Minka Kovač

dr. Nataša Toplak

dr. Sašo Čebašek

dr. Simon Koren

dr. Urška Sivka

Gregor Kovač

Lea Vukanović

Leon Korošec

mag. Anton Kovač

Marko Mitar

Matevž Miklavc

Miha Kovač

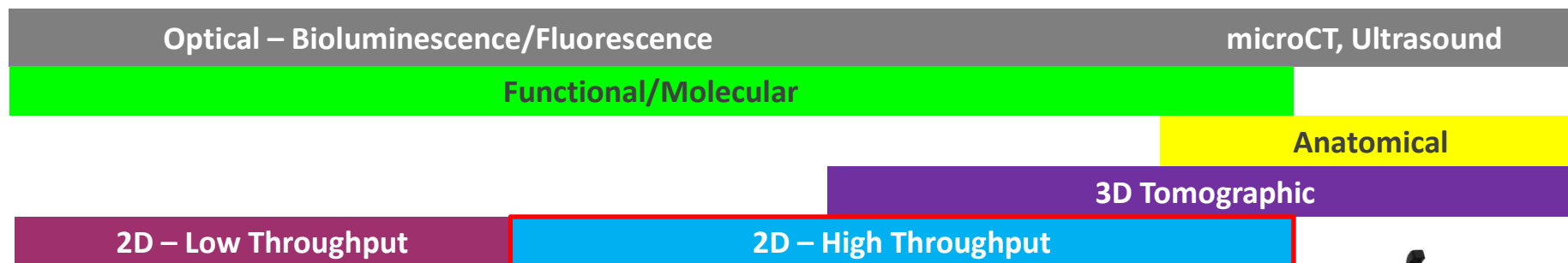
Robert Jama

Sandi Pušnik

Sandra Vrhovnik

Tine Zalokar

# PerkinElmer In Vivo Small Animal Imaging Instrument Portfolio



IVIS® Lumina™  
Platform



IVIS® Lumina S5™ and X5™



IVIS® Spectrum™  
Platform

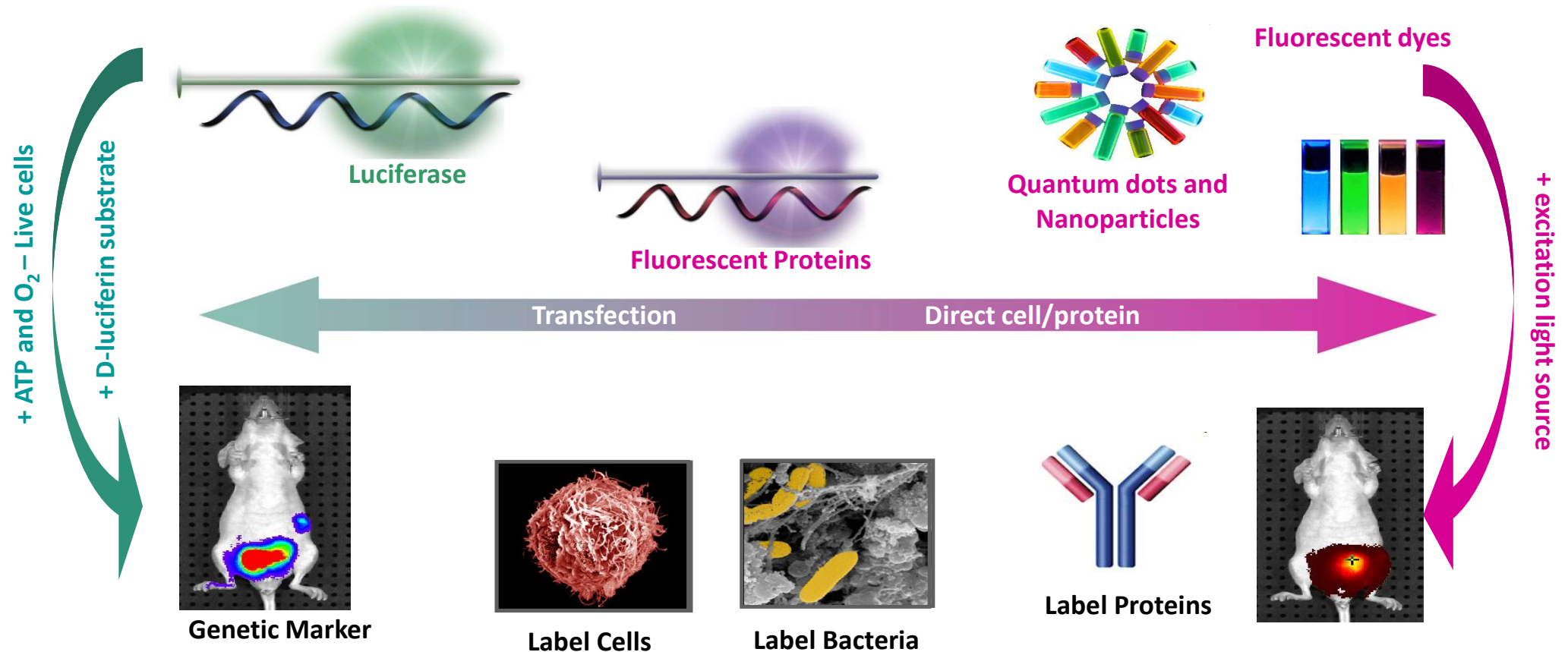


Vega®



Quantum GX2

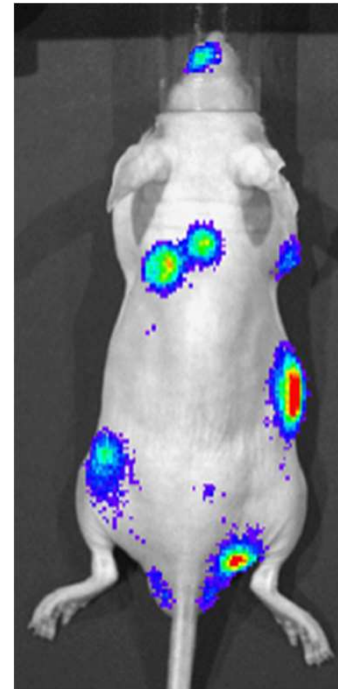
# The Power of Optical Imaging



## Why Optical Imaging?

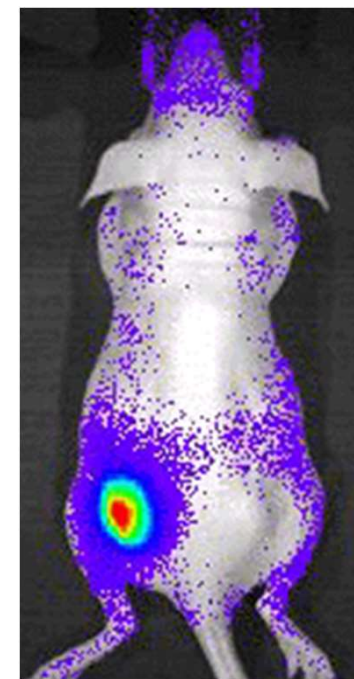
- **In vivo tracking and monitoring of tumor cells, stem cells, bacteria**
- **Study of gene function**
  - Light producing transgenic animals
- **Ideal for small animal imaging**
  - Small tissue depths
  - Relatively simple instrumentation
  - no hazardous radiation
  - easy to learn
- **Quantitative - light output is proportional to number of labeled cells**

BIOLUMINESCENCE



B16F10-luc  
melanoma  
metastases

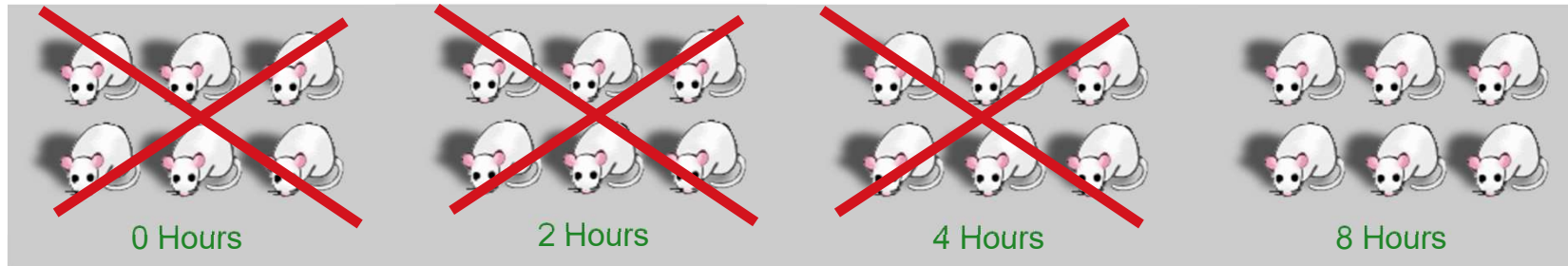
FLUORESCENCE



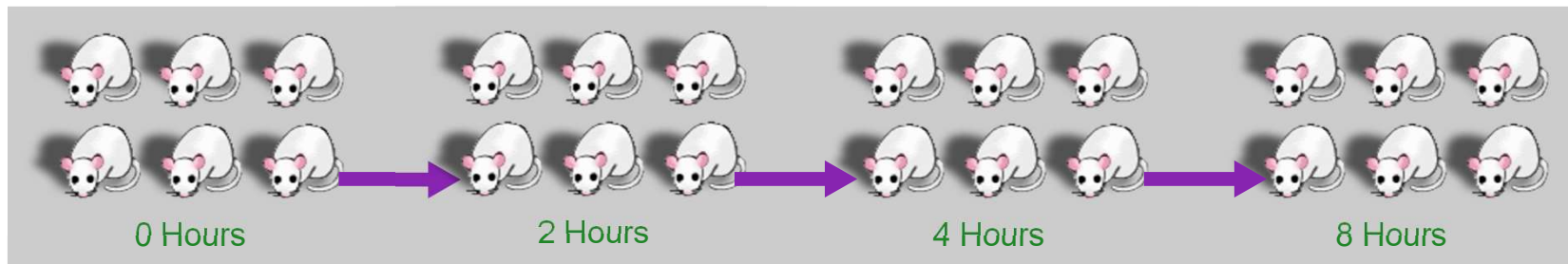
PC3M cells  
labeled with  
PKH-26 dye

# Histology vs. In Vivo Optical Imaging

CURRENT METHODOLOGY = 24 ANIMALS OVER FOUR TREATMENT POINTS



IN VIVO IMAGING METHODOLOGY = THE SAME 6 ANIMALS OVER FOUR TREATMENT POINTS



Same group of anesthetized test animals at each time point of an experiment uses far fewer animals than current methodology. By using the same set of animals at each time point yields improved statistical relevance.

Additionally: earlier and more precise detection



Any time

Since 2023

Since 2022

Since 2019

Custom range...

Sort by relevance

Sort by date

Any type

Review articles

☐ include patents

☒ include citations

☒ Create alert

[HTML] Gastrointestinal lipolysis and trans-epithelial transport of SMEDDS via oral route

[HTML] sciencedirect.com

F Xia, Z Chen, Q Zhu, J Qi, X Dong, W Zhao... - ... Pharmaceutica Sinica B, 2021 - Elsevier  
... ) in the lymph fluids was measured using the **IVIS (PerkinElmer)**. For quantification, the SMEDDSs ... The fluorescent intensities of these samples were measured with **IVIS (PerkinElmer)** to ...  
☆ Save Cite Cited by 14 Related articles All 6 versions

[PDF] Therapy targeted to the metastatic niche is effective in a model of stage IV breast cancer

[PDF] springer.com

B Yoo, A Kavishwar, P Wang, A Ross, P Pantazopoulos... - Scientific reports, 2017 - Springer  
Abstract Treatment of stage IV metastatic breast cancer patients is limited to palliative options and represents an unmet clinical need. Here, we demonstrate that pharmacological ...  
☆ Save Cite Cited by 41 Related articles All 11 versions

Sonodynamic therapy on intracranial glioblastoma xenografts using sinoporphyrin sodium delivered by ultrasound with microbubbles

Z Pi, Y Huang, Y Shen, X Zeng, Y Hu, T Chen... - Annals of Biomedical ..., 2019 - Springer  
... analyzed by a Xenogen **IVIS** spectrum system (**IVIS SPECTRUM**; **PerkinElmer** Inc., Waltham, ... DVDMS was detected using an **IVIS** imaging system (**PerkinElmer** Inc., Waltham, MA, USA). ...  
☆ Save Cite Cited by 34 Related articles All 5 versions

Combining miR-10b-Targeted Nanotherapy with Low-Dose Doxorubicin Elicits Durable Regressions of Metastatic Breast CancerRegression of Metastatic Cancer ...

[HTML] nih.gov

B Yoo, A Kavishwar, A Ross, P Wang, DP Tabassum... - Cancer research, 2015 - AACR  
... an **IVIS** Spectrum imaging station (**Perkin Elmer**) for the reconstruction of 3-dimensional fluorescence imaging tomography (3D-FLIT) using Living Image software (ver. 4.4, **Perkin Elmer**)...  
☆ Save Cite Cited by 63 Related articles All 8 versions

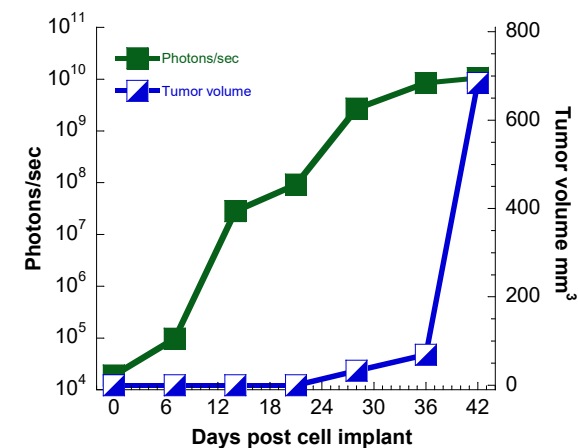
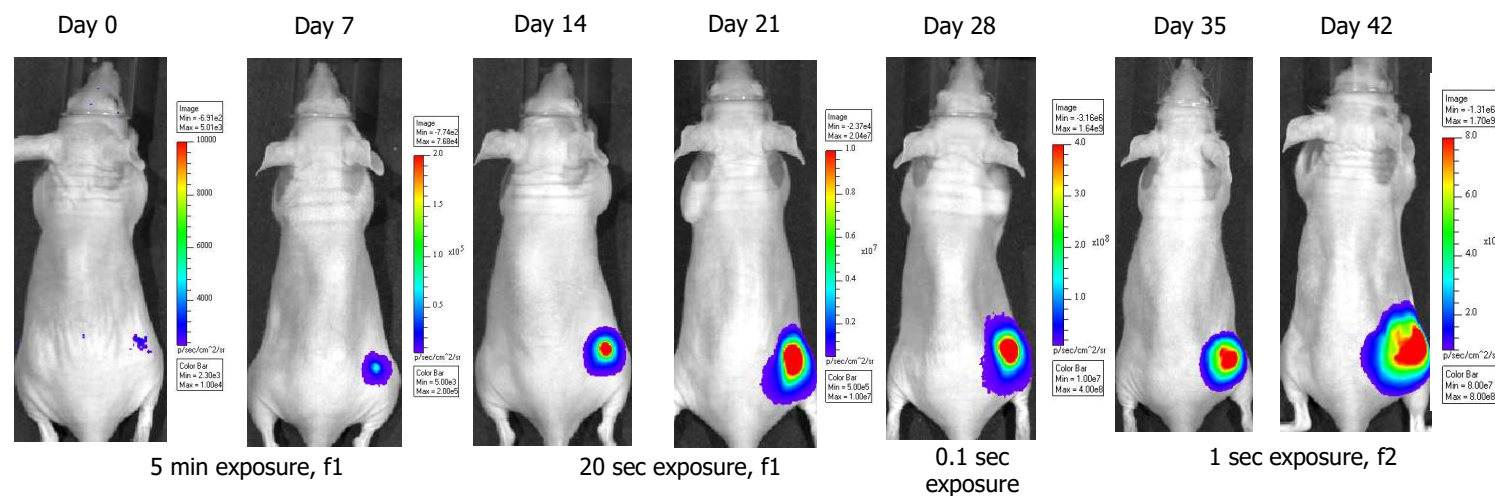


## Luminescence - Cell Tracking



# Quantifying Tumor Growth with Bioluminescent Cell Lines

## LONGITUDINAL STUDIES REQUIRE CALIBRATION IN PHYSICAL UNITS



- Five 4T1-luc2-1A4 cells injected on day 0 in a nu/nu mouse

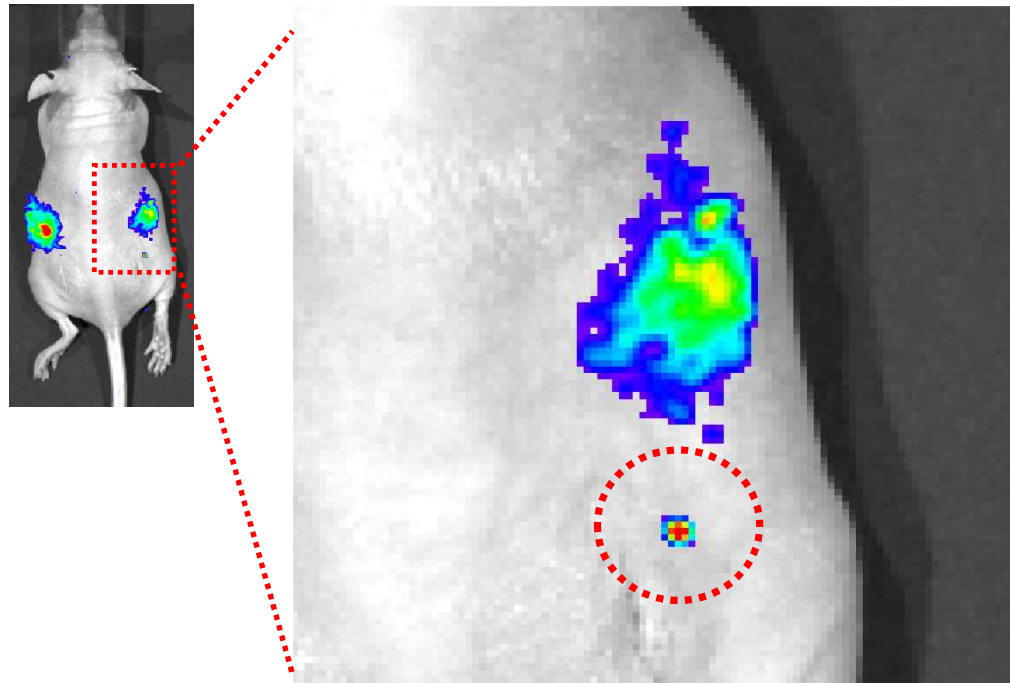
## Brightness of Revvity Cell Lines

HT1080-Red-Fluc	Human <b>Fibrosarcoma</b> Cancer Cell line.	> 30,000 p/s/c	BW 128092
4T1-Red-Fluc	Murine <b>Breast Cancer</b> Cell line	> 15,000 p/s/c	BW 124087
MDA-MB-231-Red-Fluc	Human <b>Breast Cancer</b> Cell line, ideal for experimental metastasis model	> 4,000 p/s/c	BW 124319
GL261-Red-Fluc	Murine <b>Glioma</b> Cell line	> 15,000 p/s/c	BW 134246
HepG2-Red-Fluc	Human <b>Hepatic Cancer</b> cell line	> 35,000 p/s/c	BW 134280
PC-3M-Red-Fluc	Human <b>Prostate Cancer</b> Cell line, orthotopic, intracardiac tumor models	> 30,000 p/s/c	BW 124089
PC-3-Red-Fluc	Human <b>Prostate Cancer</b> Cell line	> 30,000 p/s/c	BW 128444
LnCaP-Red-Fluc	Human <b>Prostate Cancer</b> Cell line	> 3,000 p/s/c	BW 125055
B16-F10-Red-Fluc	Murine <b>Melanoma</b> Cancer Cell line	> 6,000 p/s/c	BW 124734
HCT-116-Red-Fluc	Human <b>Colorectal Cancer</b> Cell line	> 4,000 p/s/c	BW 124318
HT-29-Red-Fluc	Human <b>Colorectal Cancer</b> Cell line	> 30,000 p/s/c	BW 124353
Colo205-Red-Fluc	Human <b>Colorectal Cancer</b> Cell line	> 6,000 p/s/c	BW 124317
U-87 MG-Red-Fluc	Human <b>Brain Cancer</b> Cell line, ideal for glioblastoma models	> 8,000 p/s/c	BW 124577
NCI-H460-Red-Fluc	Human <b>Lung Cancer</b> Cell line, ideal for orthotopic lung tumor models	> 4,000 p/s/c	BW 124316
K-562-Red-Fluc	Human <b>Leukemia</b> Cell line	> 4,000 p/s/c	BW 124735
BxPC3-Red-Fluc	Human <b>Pancreatic Cancer</b> Cell	> 15,000 p/s/c	BW 125058
MCF-7-Red-Fluc	Human <b>Breast Cancer</b>	> 10,000 p/s/c	BW 119262
A549-Red-Fluc	Human <b>Lung Cancer</b>	> 25,000 p/s/c	BW 119266
LL/2-Red-Fluc	Murine <b>Lung Cancer</b>	> 5,000 p/s/c	BW 119267
SKOV3-Red-Fluc	Human <b>Ovarian Cancer</b>	> 10,000 p/s/c	BW 119276
4T1-Red-Fluc-GFP	Murine <b>Breast cancer</b> cell line dual labeled with Luciferase and GFP	> 15,000 p/s/c	BW 128090
MDA-MB-231-Red-Fluc-GFP	Human <b>Breast cancer</b> cell line dual labeled with Luciferase and GFP	> 10,000 p/s/c	BW 128442
PC-3-Red-Fluc-GFP	Human <b>Prostate cancer</b> cell line dual labeled with Luciferase and GFP	> 8,000 p/s/c	BW 133416

## Non-invasive imaging of a single 4T1-luc2 cell in nu/nu mouse

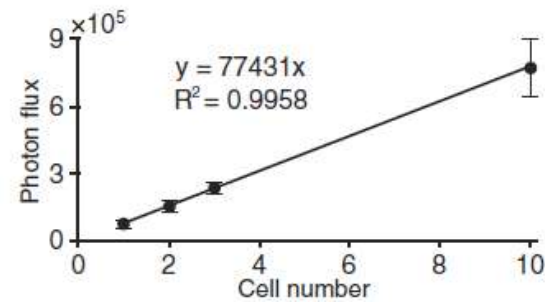
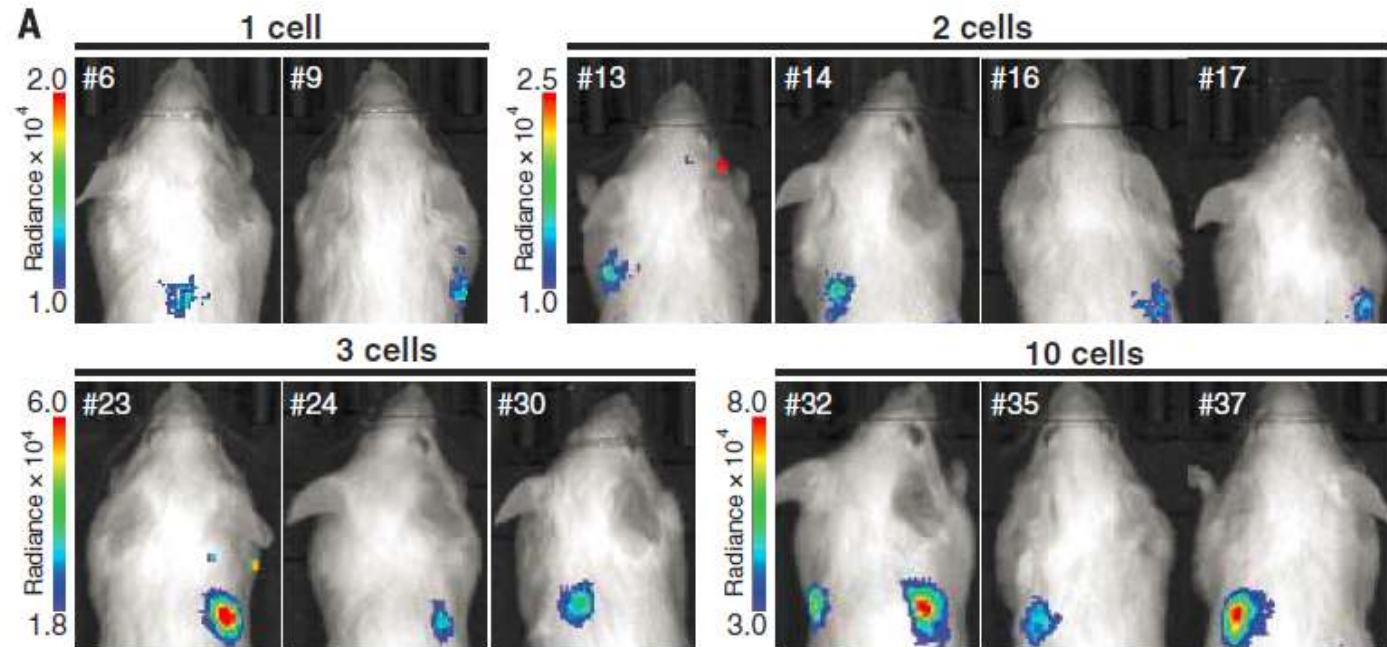
4T1: ADENOCARCINOMA CELLS – 6500 PHOTONS/S/CELL

Transduced using lentivirus containing luciferase 2 gene under the control of human ubiquitin C promoter



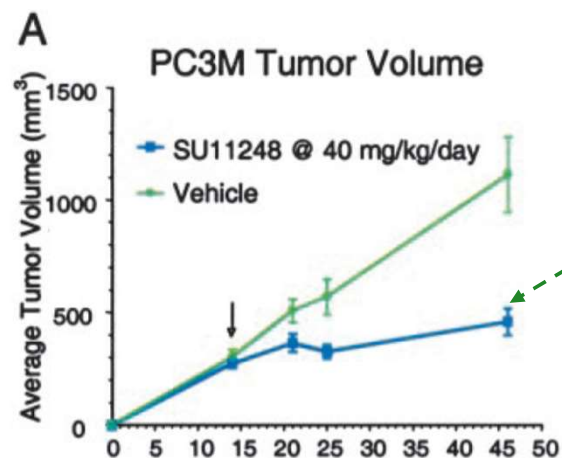
# Deep Tissue Imaging with AkaLumine and AkaLuc

Detection of bioluminescence from a small number of AkaLuc-expressing HeLa cells trapped in the mouse lung.

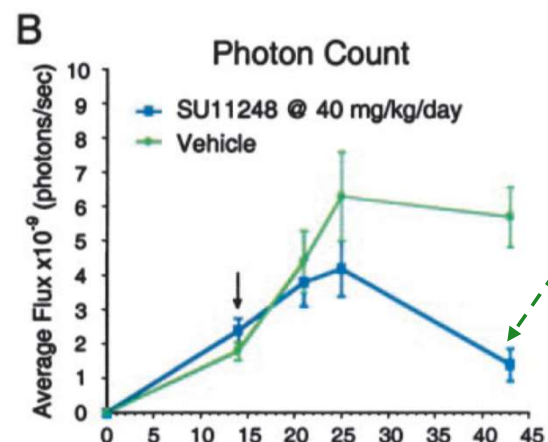




# Sutent – Fast Tracked FDA Approval

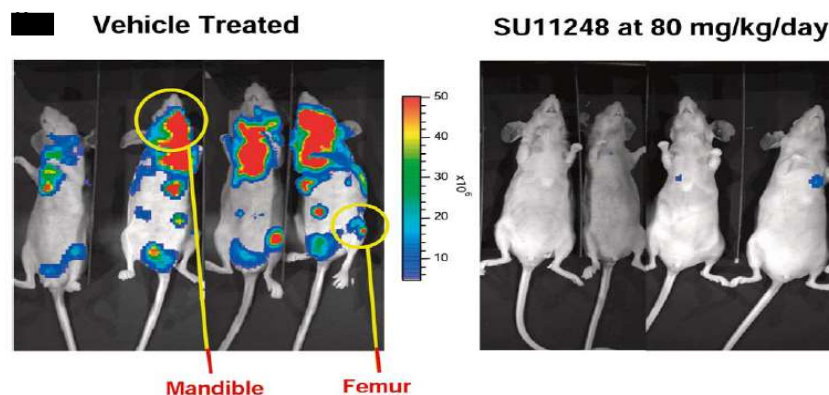


**Physical measurement**  
(tumor still getting bigger)



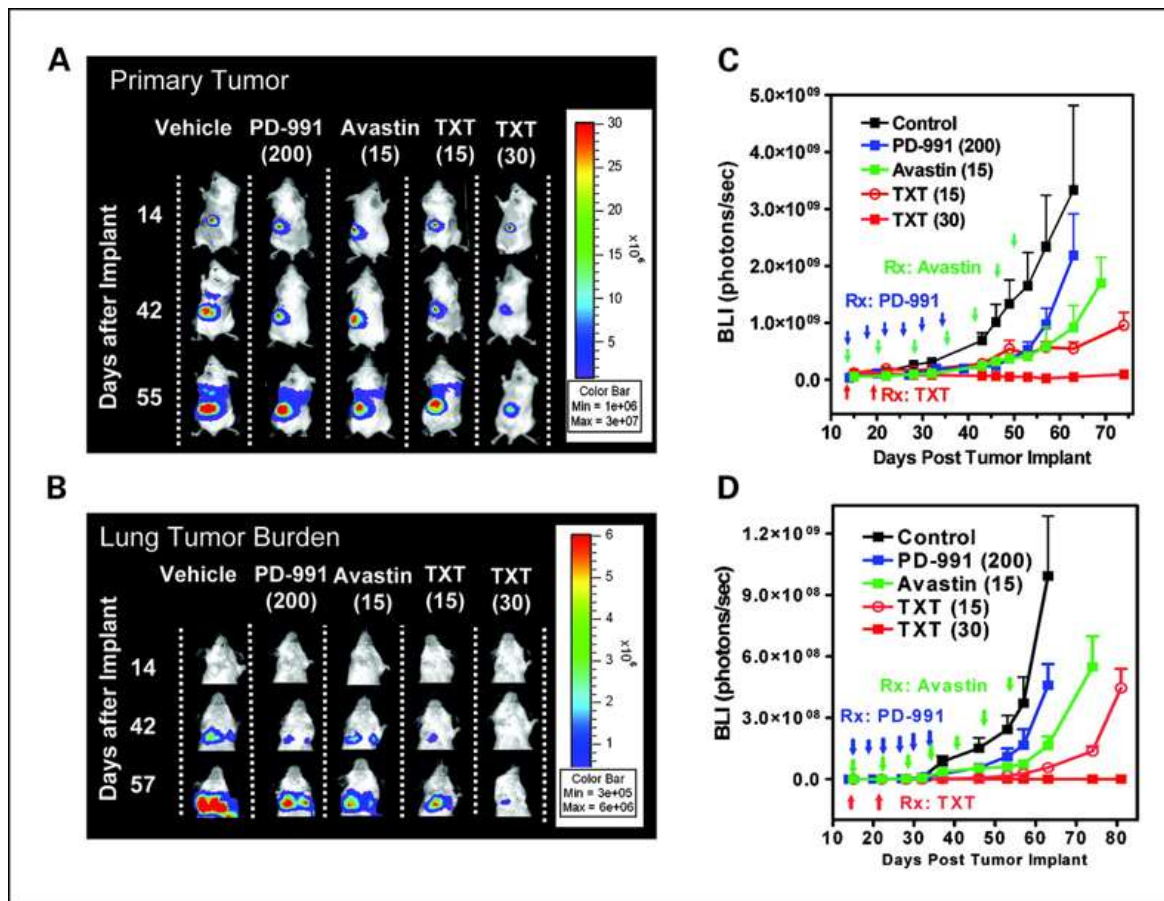
**Biophotonic imaging**  
(tumor cells being killed)

Mendel *et al* 2003



Murray *et al* 2003

# Therapeutic Development in a SRC Implantation Model



## BENEFITS

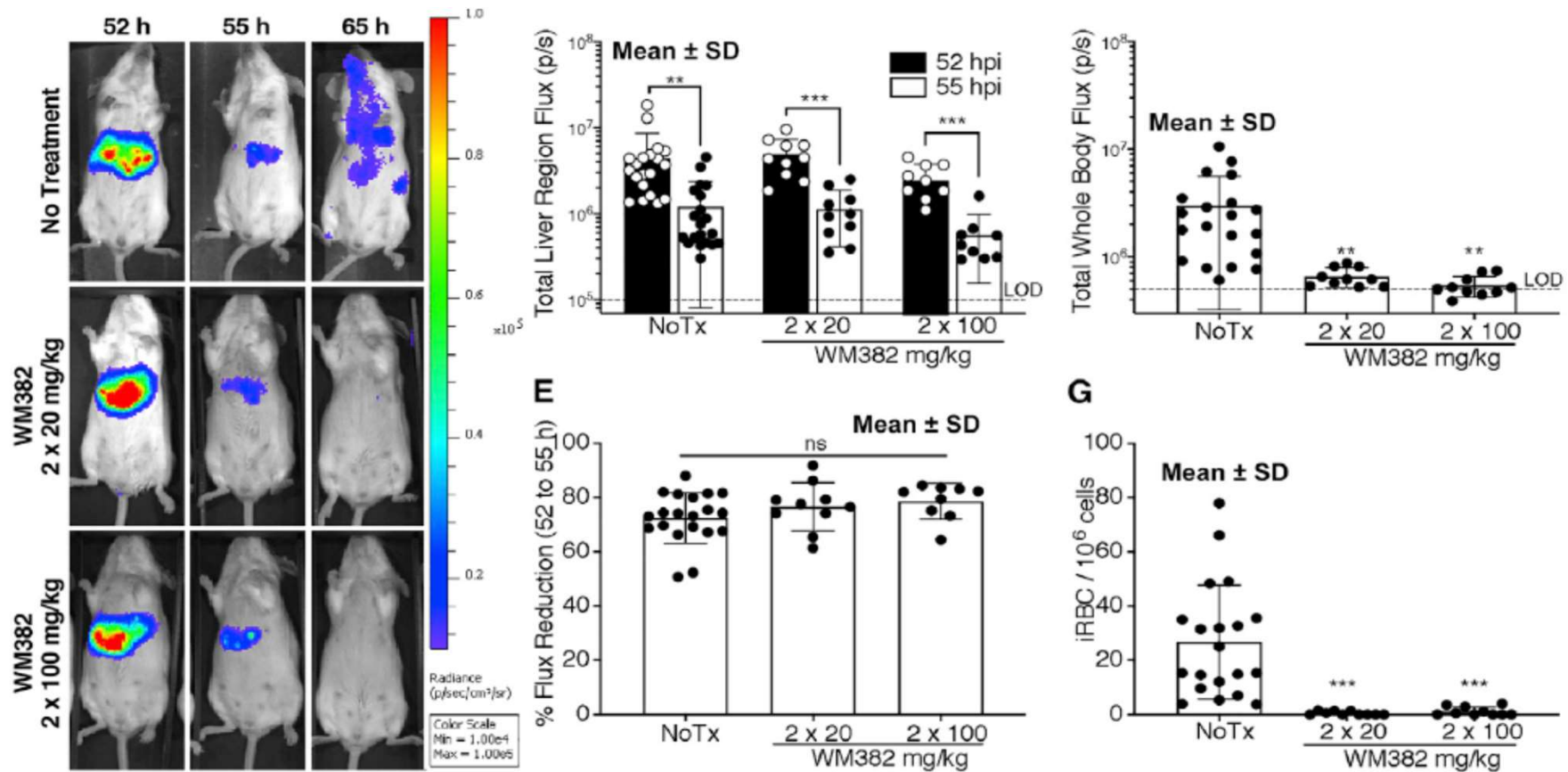
- Expedites progress towards clinical trials
- Measurable economic benefits include reduced animal costs and personnel
- Simultaneous insights into drug efficacy, kinetics, target, mechanism
- Superior statistics and data reproducibility

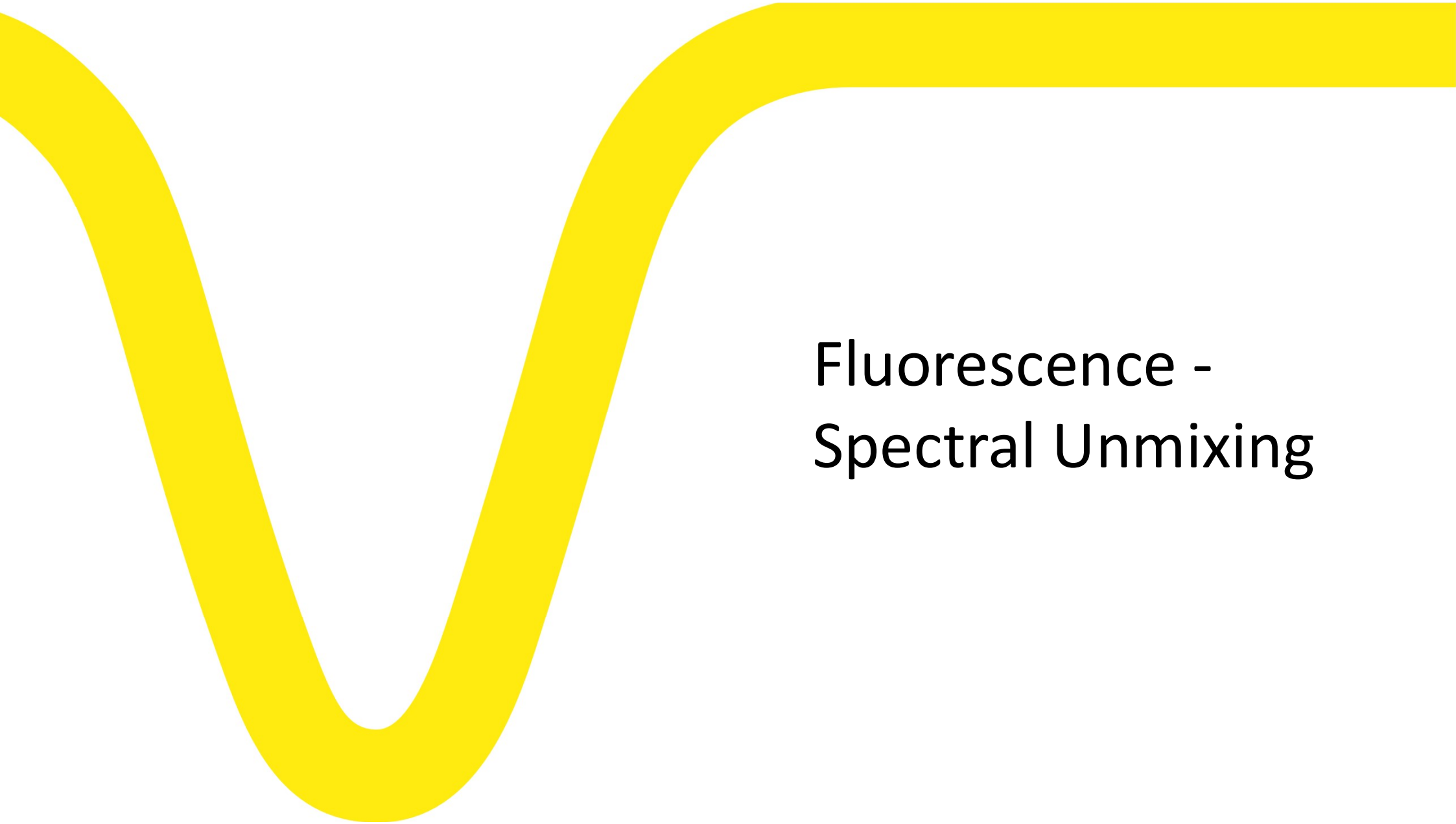




# Luminescence - Infectious Diseases

# In Vivo Imaging Shows Inhibition of *P. falciparum* Blood Stage

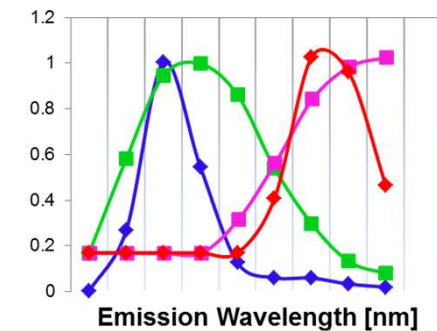
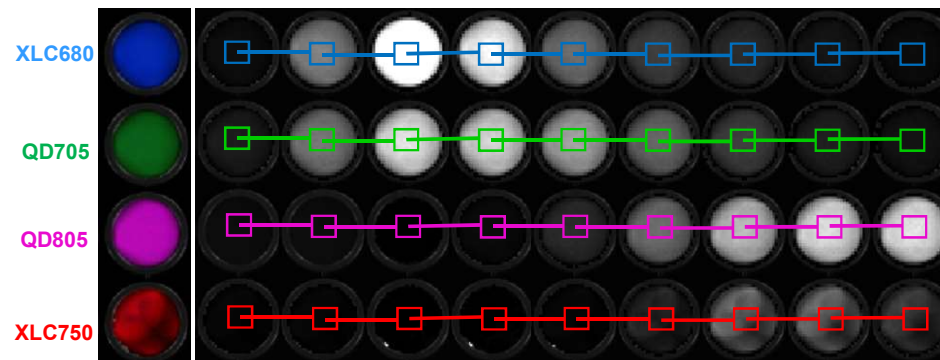




# Fluorescence - Spectral Unmixing

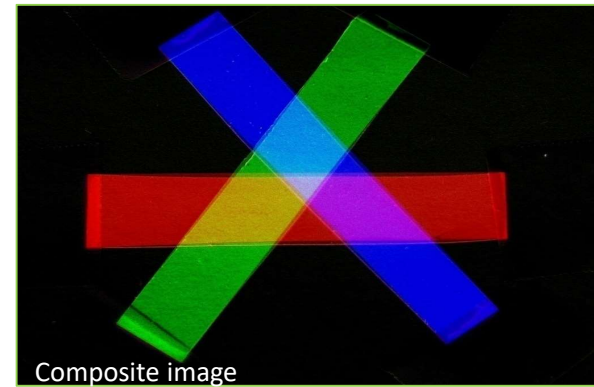
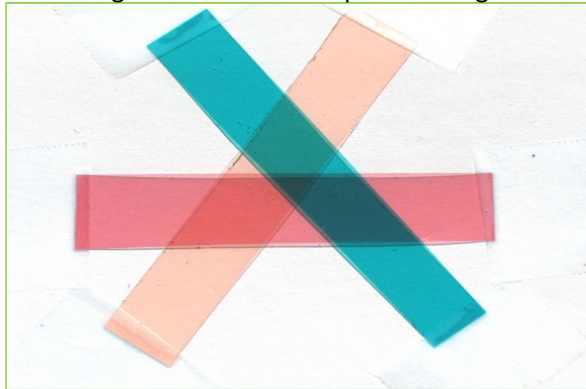
# Spectral Imaging is Essential for Spectral Unmixing

- IMAGES ACQUIRED AT MULTIPLE WAVELENGTHS FOR A SPECTRAL SCAN (EVERY 20 nm)
- BUILDING A SPECTRAL LIBRARY

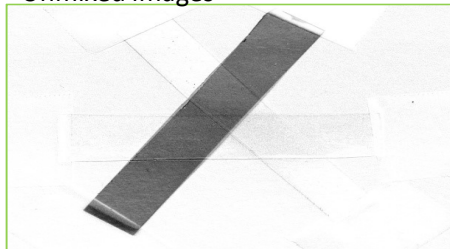


## How is Spectral Unmixing accomplished?

RGB image calculated from spectral image data



Unmixed images

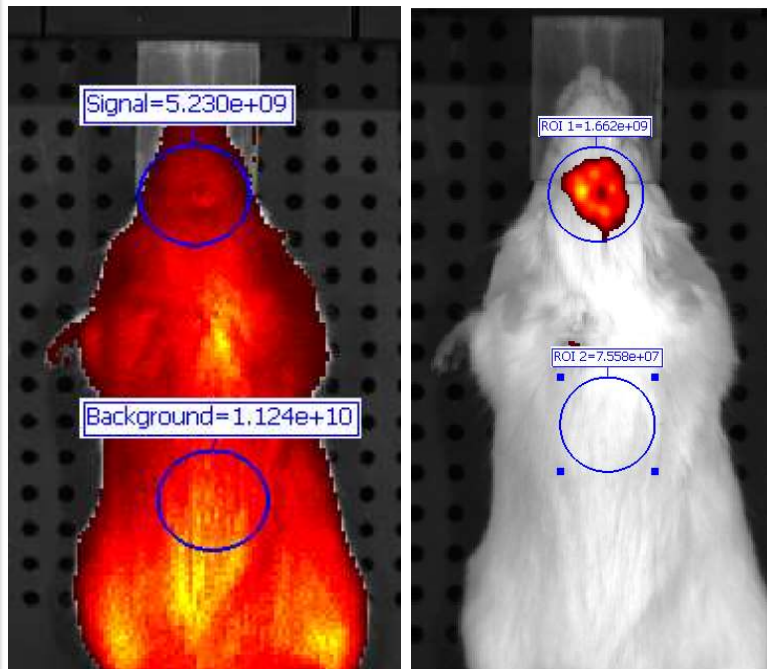


## When is Spectral Unmixing Most Useful?

Reduce Autofluorescence to  
Increase Signal to Noise

S/N = .46

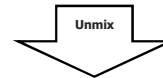
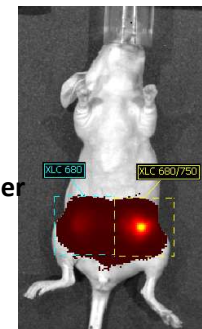
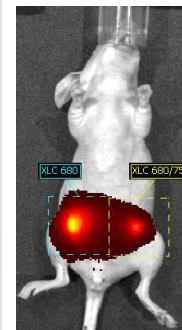
Unmixed S/N = 22



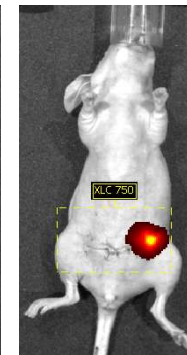
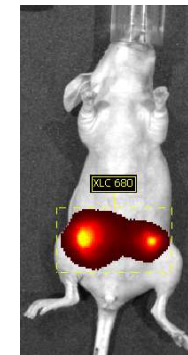
Separate Colocalized Components

XLC 680 left and right  
XLC 750 right

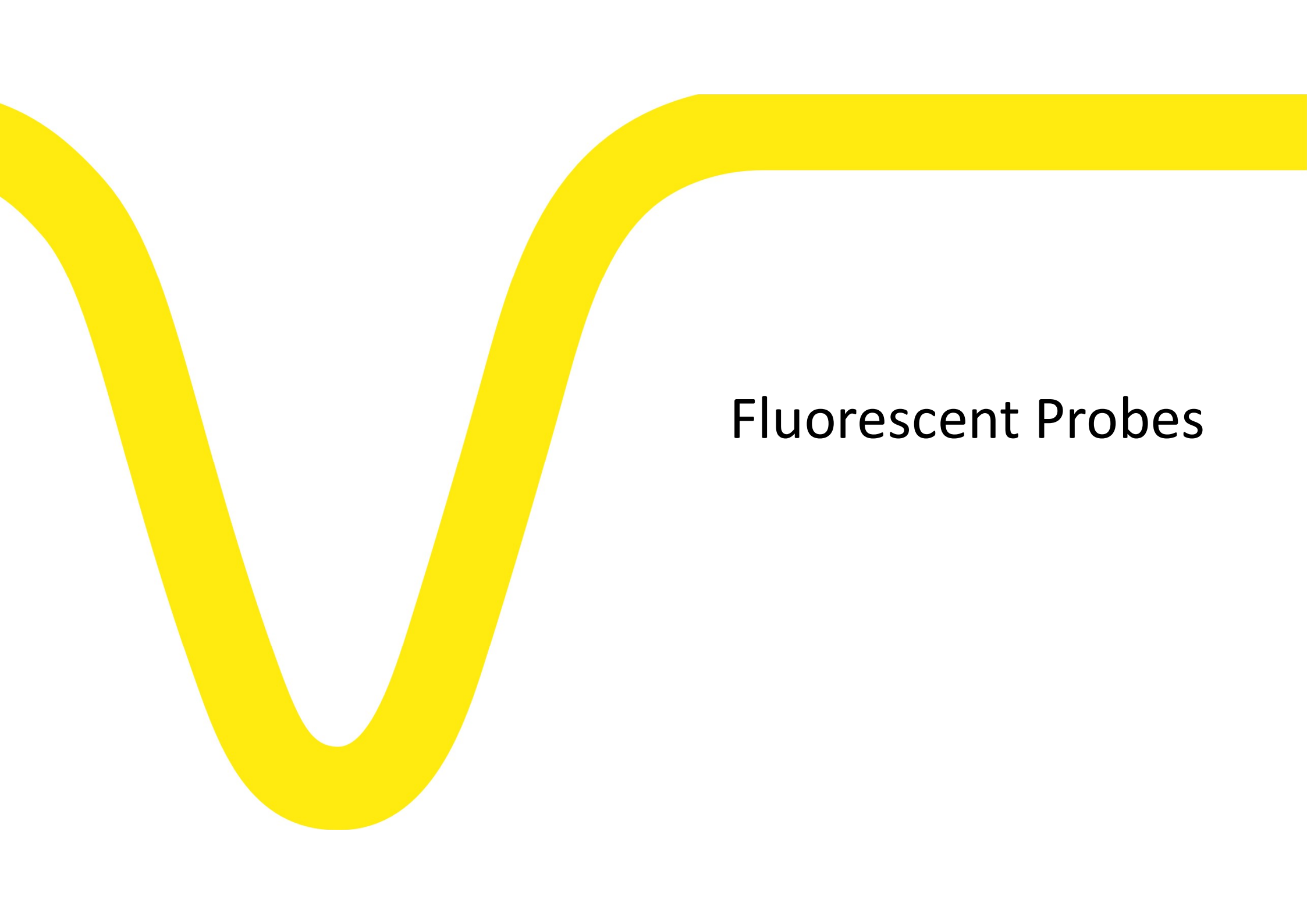
Signals indistinguishable  
Significant overlap



Quantification of Individual Components Possible



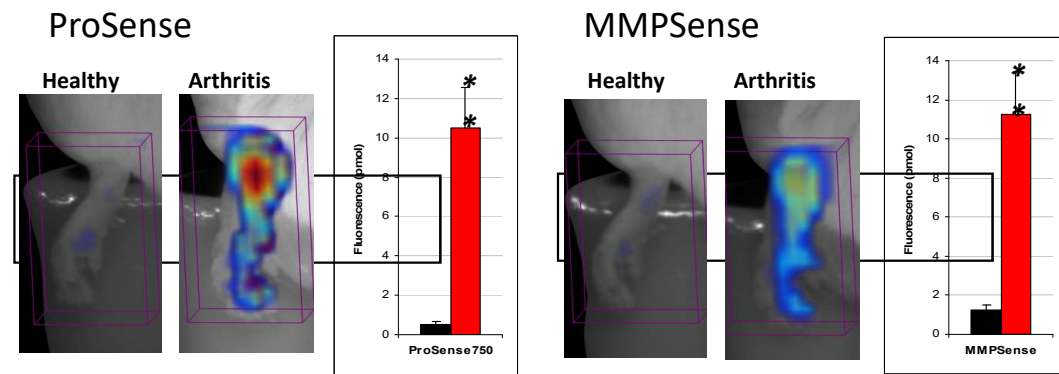




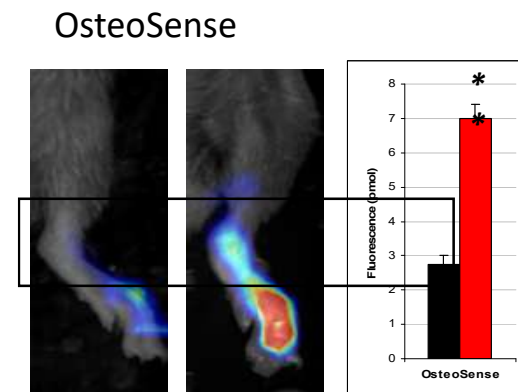
Fluorescent Probes

# Different Revvity Agents for Imaging Arthritis Biology

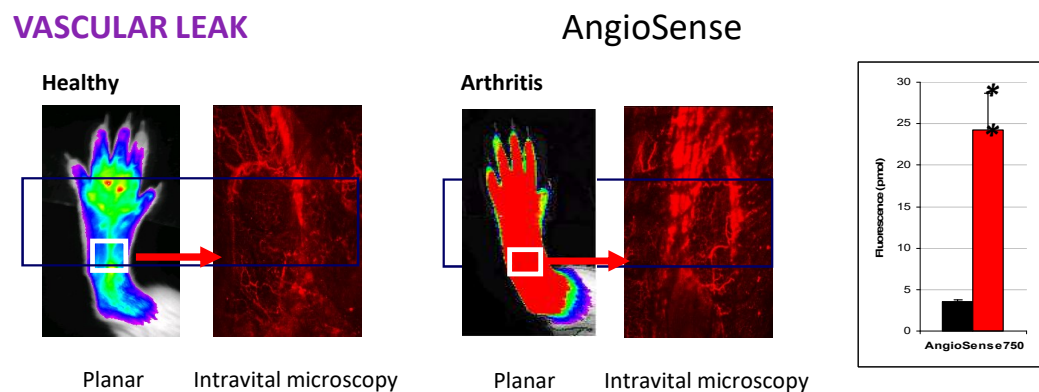
## INFLAMMATION PROTEASE ACTIVITY



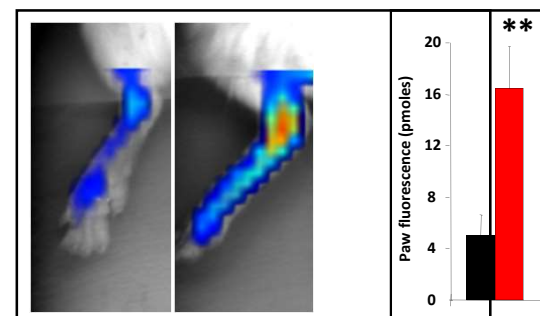
## BONE CHANGES



## VASCULAR LEAK

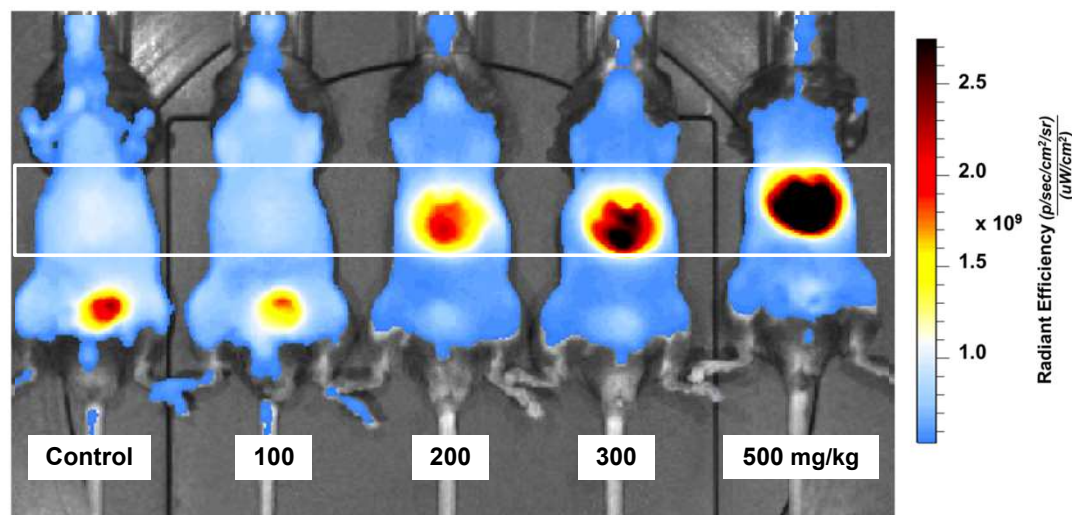


## Cat K FAST 680

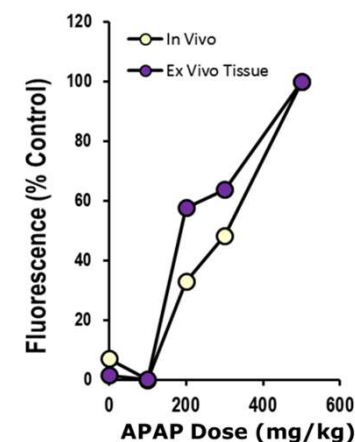


# Toxicology Imaging: Drug Induced Liver Injury

## IN VIVO IMAGING

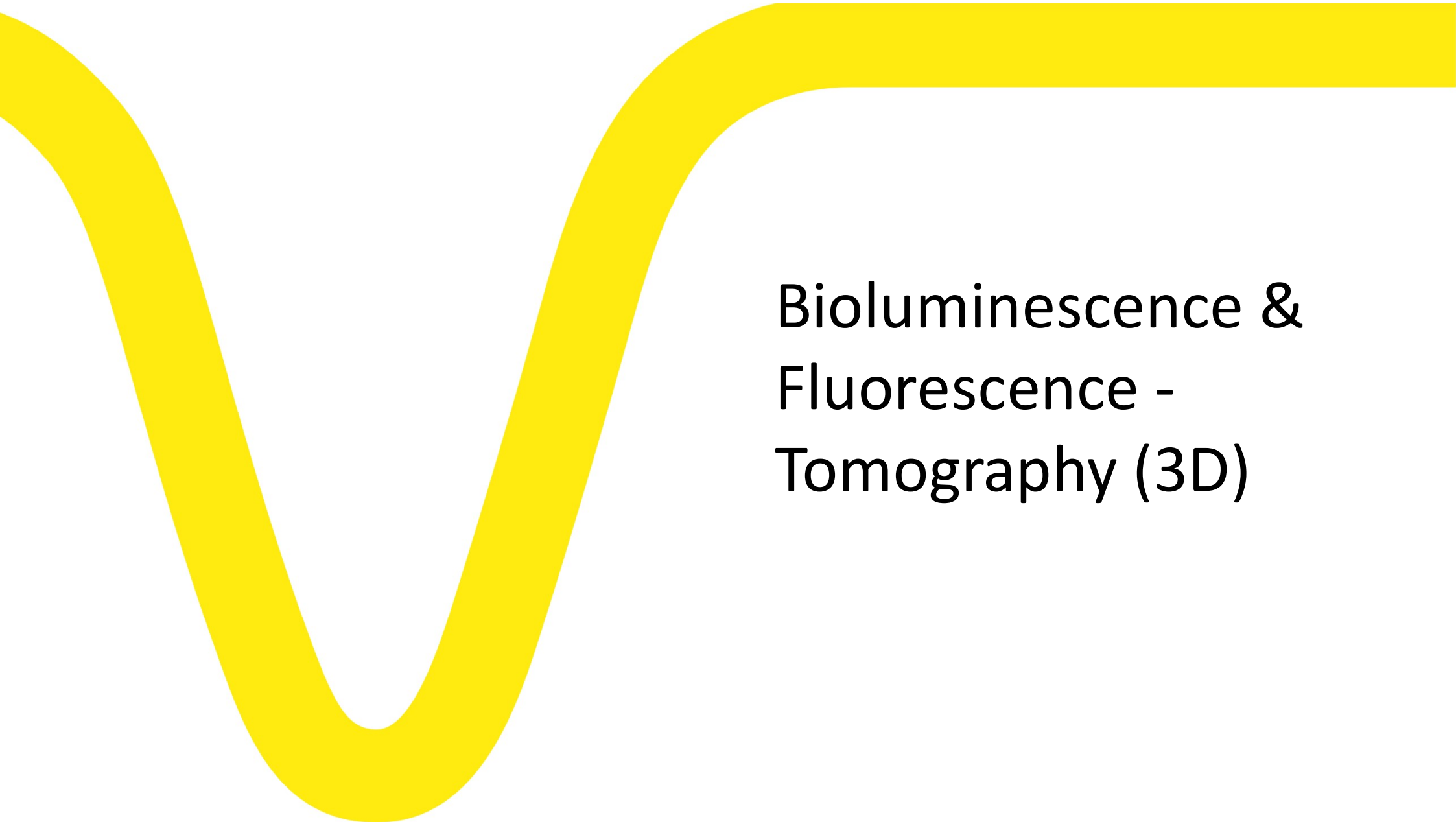


## C. Imaging Quantification



## Dose-responsive effects of Acetaminophen/Paracetamol on **Annexin-Vivo 750** accumulation in the liver

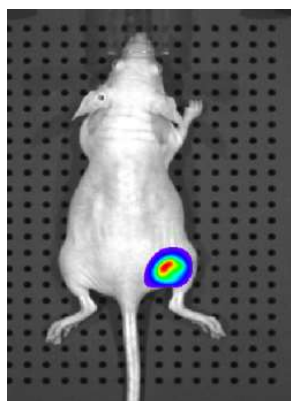
- Normal Annexin-Vivo 750 kidney/bladder clearance altered with increased phosphatidyl serine exposure in the liver
- Ex vivo tissue FL intensity correlates well with in vivo imaging, supporting a robust non-invasive approach to imaging liver tox



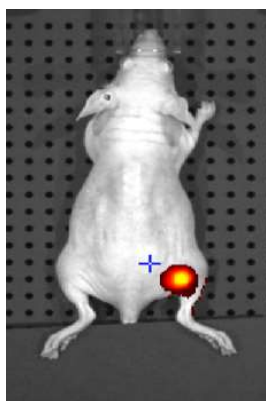
# Bioluminescence & Fluorescence - Tomography (3D)

# Imaging MMP Activity in Mammary Tumors

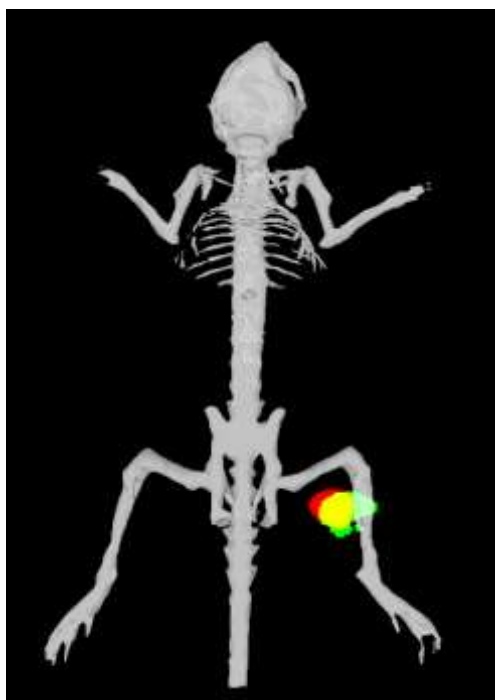
## FLANK IMPLANTATION OF MD231 TUMOR TARGETED WITH MMPSENSE680



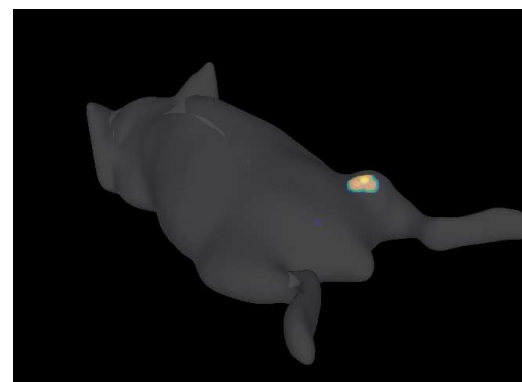
Bioluminescence



Fluorescence



Tomographic Bioluminescence & Fluorescence co-registered with the mouse atlas



Reconstruction with animal surface rendering

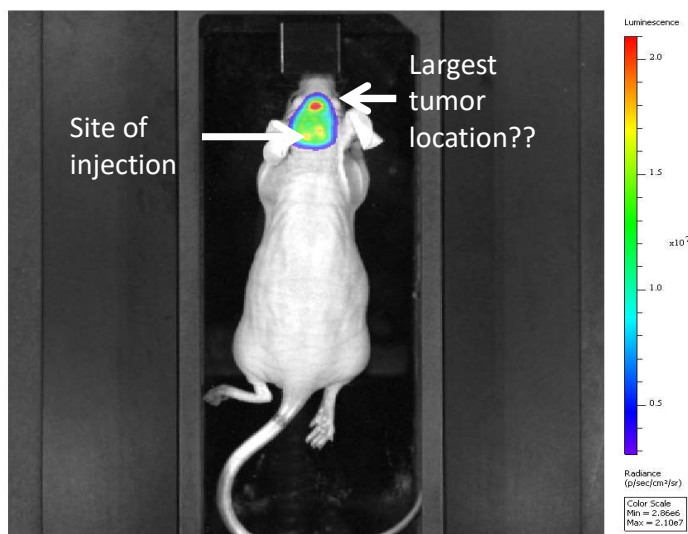
## Mouse Imaging Shuttle for Co-Registration



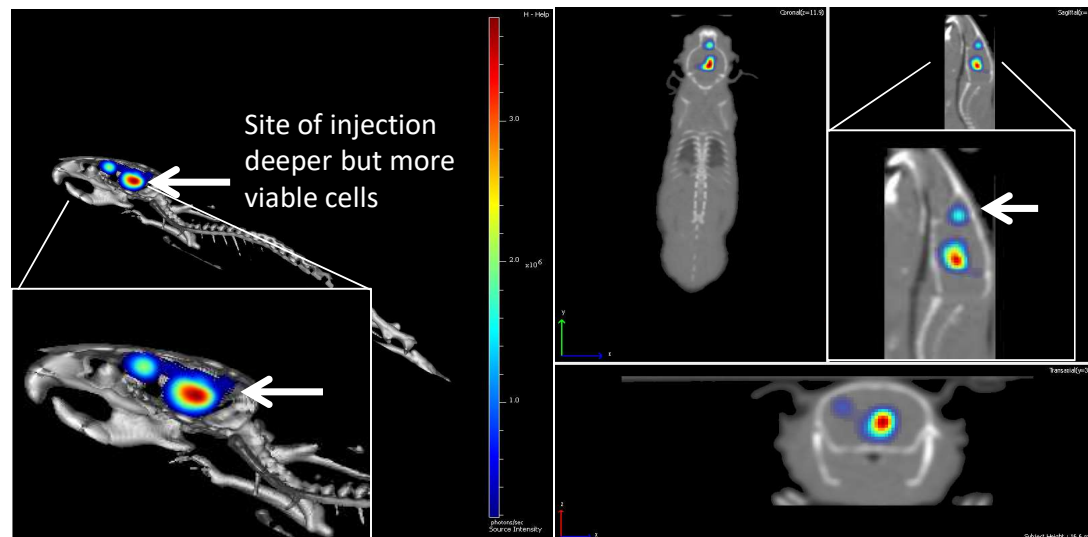


# Brain Tumor Model – Absolute Quantification

2 D



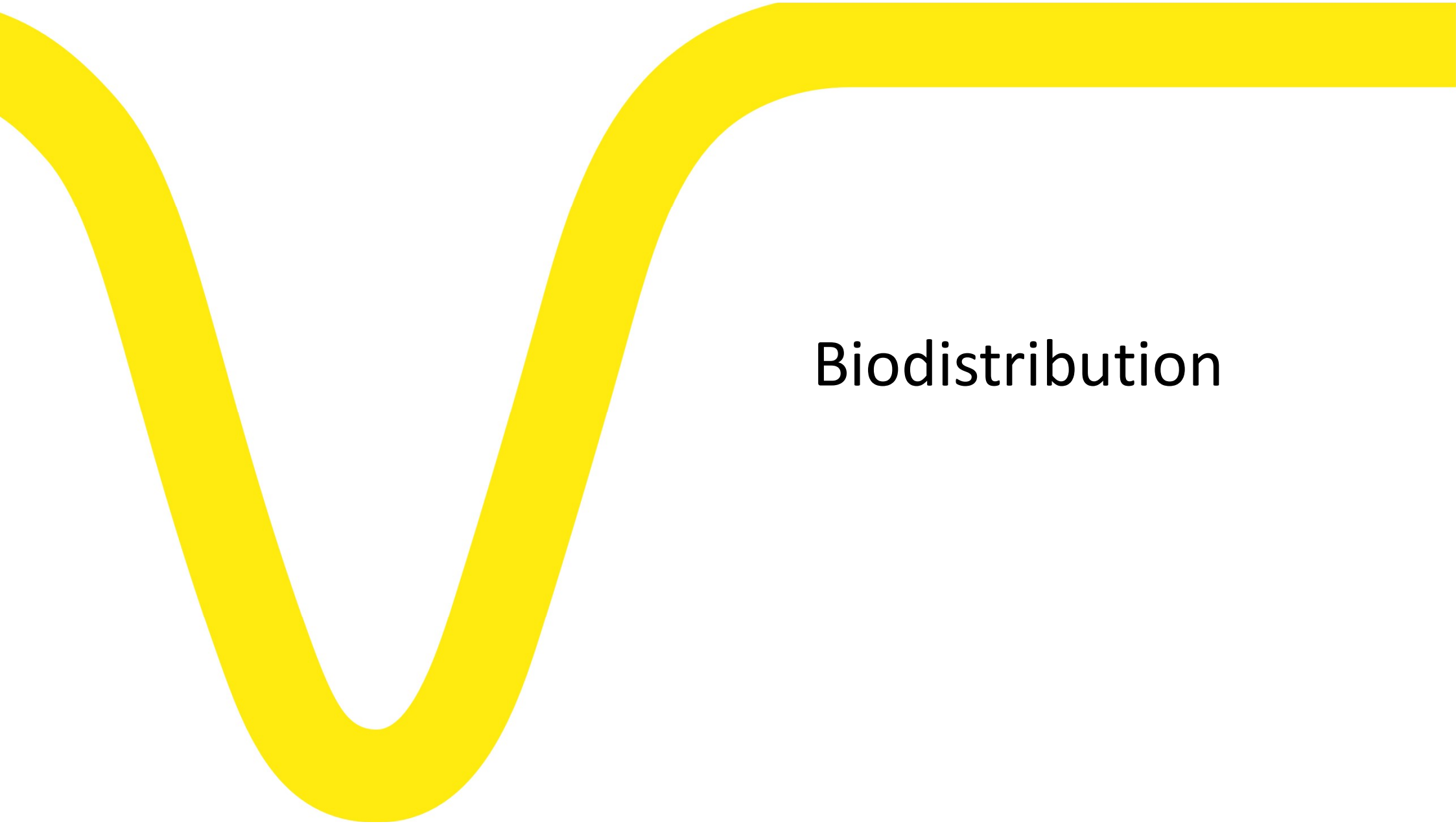
3 D



Metastatic lesion shallower thus more intense in 2D however fewer viable cells

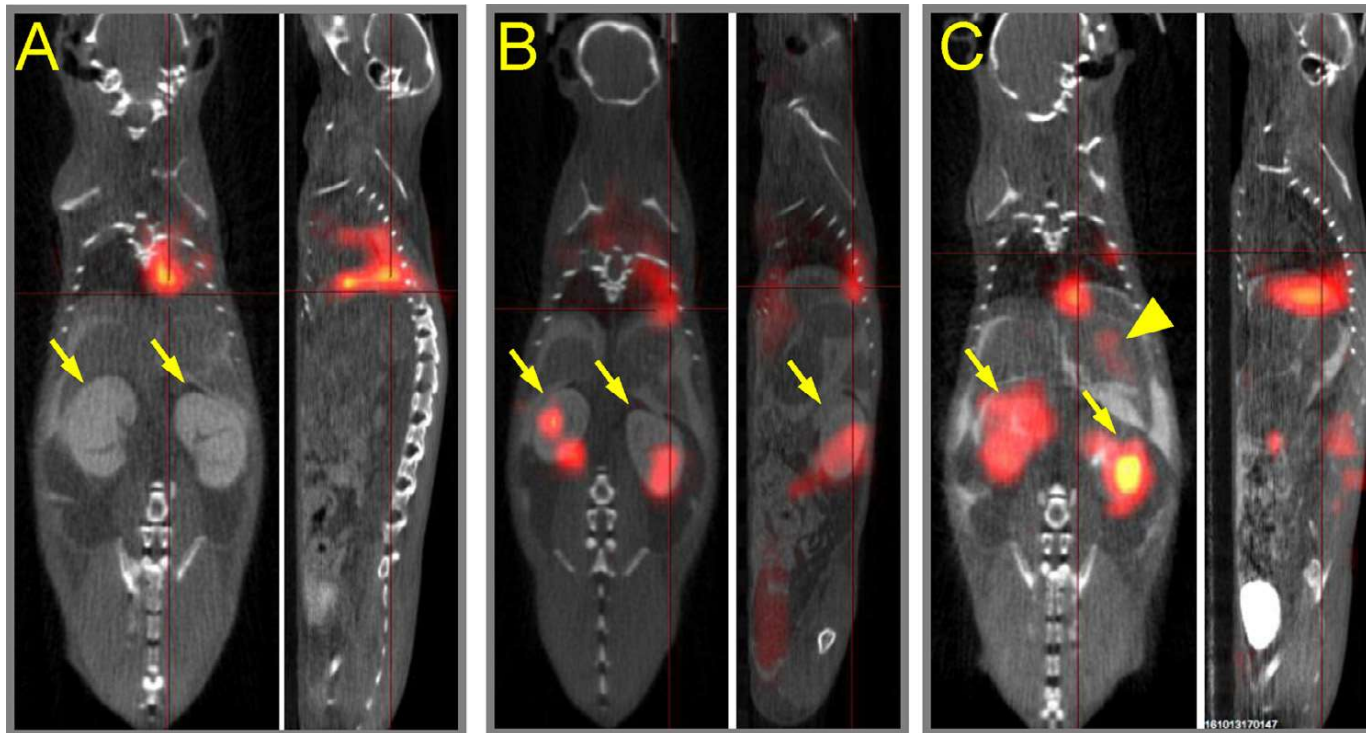
- 2D acquisition excels at quick high through-put quantitation over time accurately determining growth, viability and efficacy
- However focal points of signal are dependent on depth of source

- 3D analysis factors in attenuation, scattering, and diffusion
- Pixels clustered based on resultant emission curve thus elucidating differences in depth and intensity more accurately
- 3D imaging can shed light on both pinpoint localization and depth of source
- Resultant data more representative of actual tumor locations in brain
- Individual tumor locations can be monitored with ease



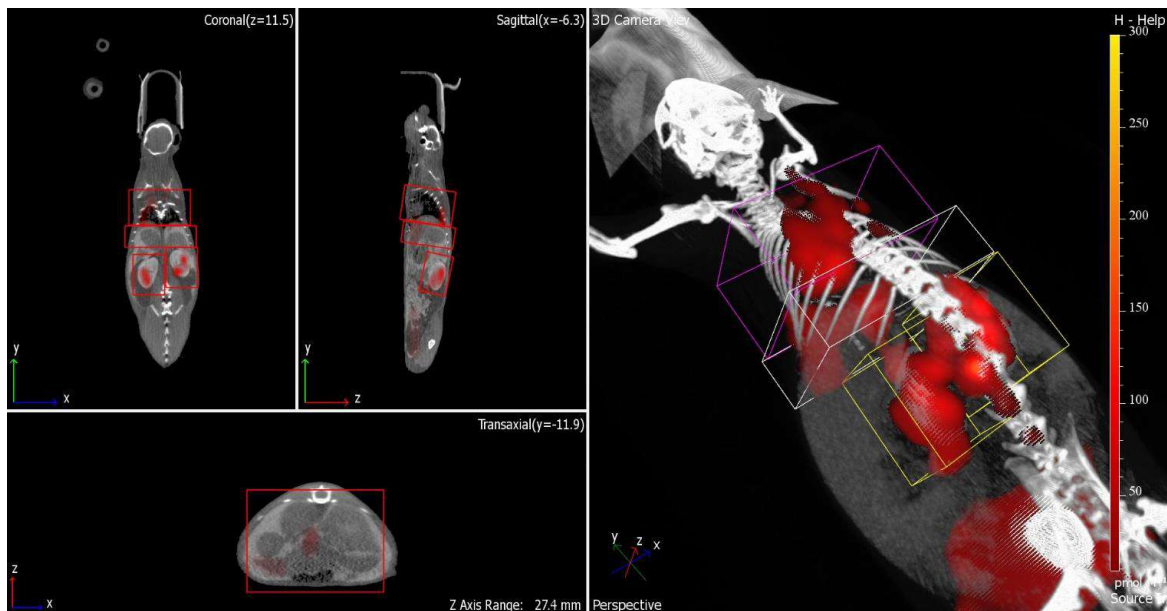
Biodistribution

## Biodistribution of siRNA after Intratracheal Application in Mice

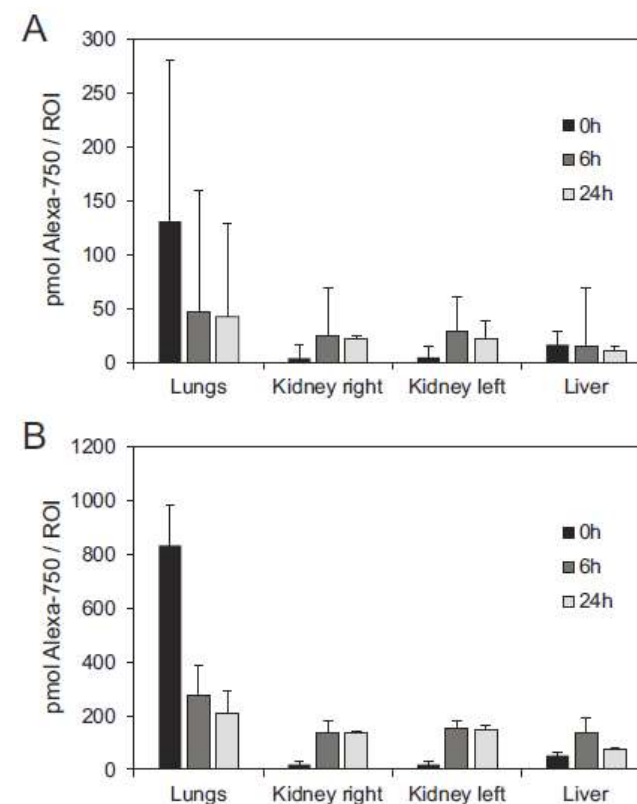


CT/FLIT IMAGING OF AF750-siRNA BIODISTRIBUTION BALB/C MICE

# Biodistribution of siRNA after Intratracheal Application in Mice



CT/FLIT IMAGING OF AF750-siRNA BIODISTRIBUTION BALB/C MICE

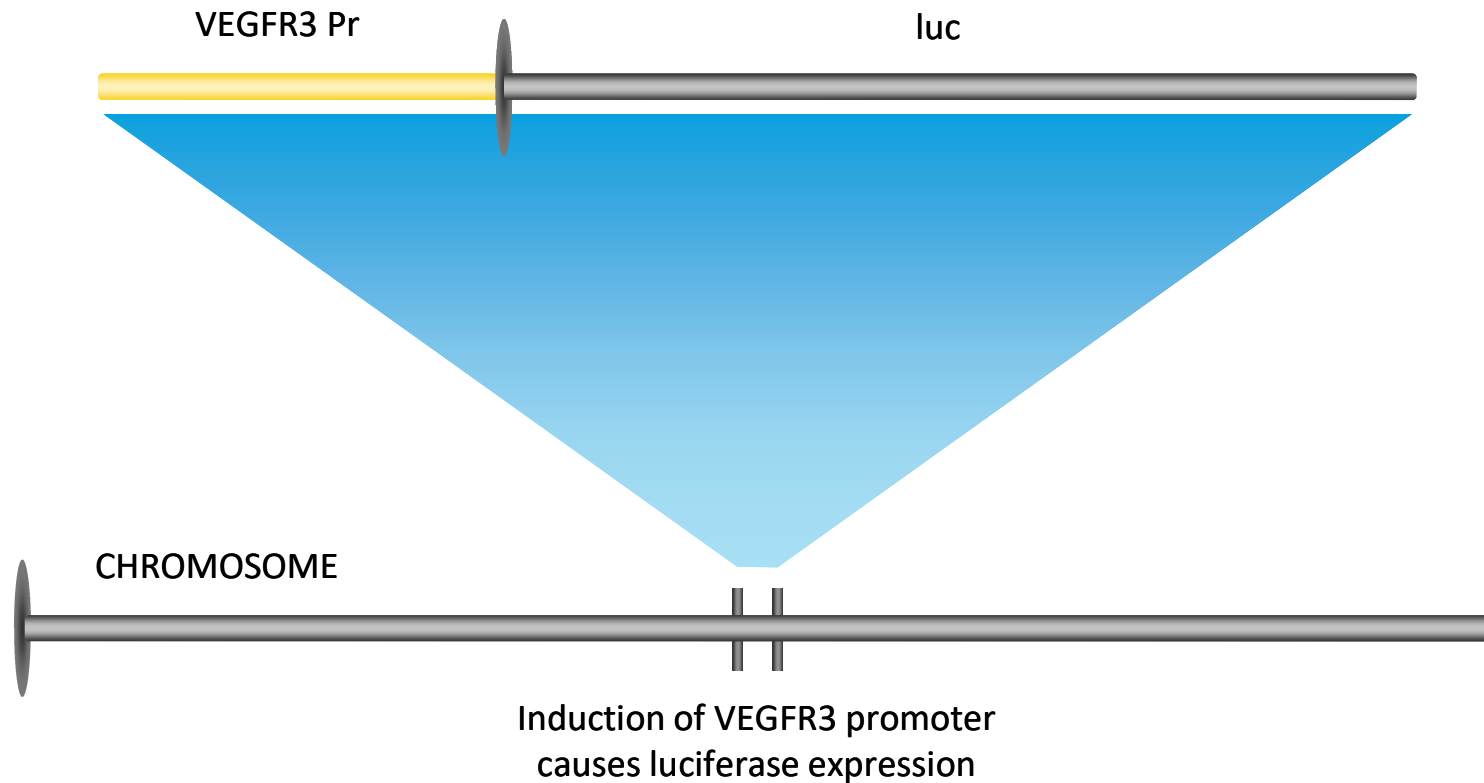


Molecular quantification of AF750 labeled siRNA by FLIT  
A: 2.5 μg      B: 10 μg



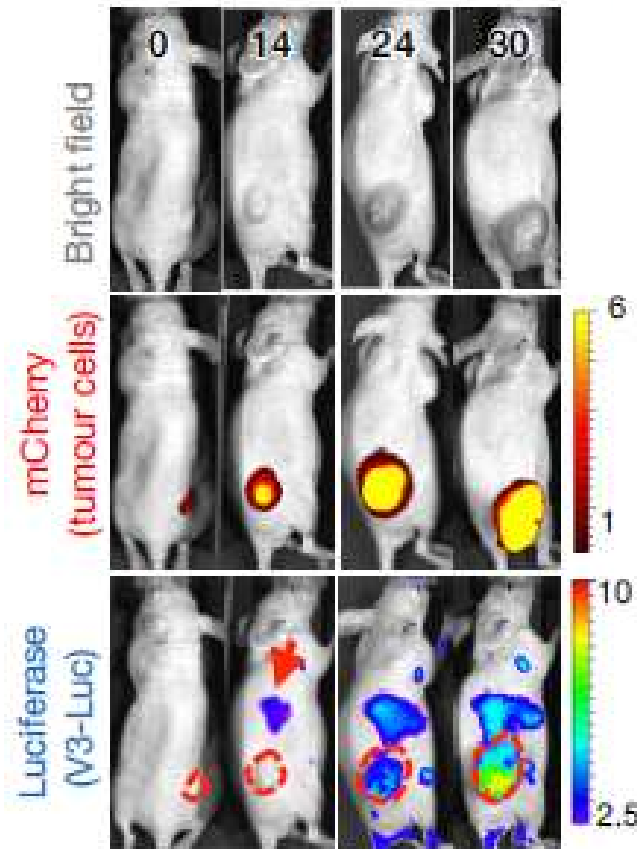
# Transgenic Animals – Molecular Mechanisms

## Transgenic Animals: Vascular Endothelial Cell Growth Factor Receptor 3





## Vegfr3<sup>Luc</sup> Reporter Mice for Imaging of Neo-Lymphangiogenesis



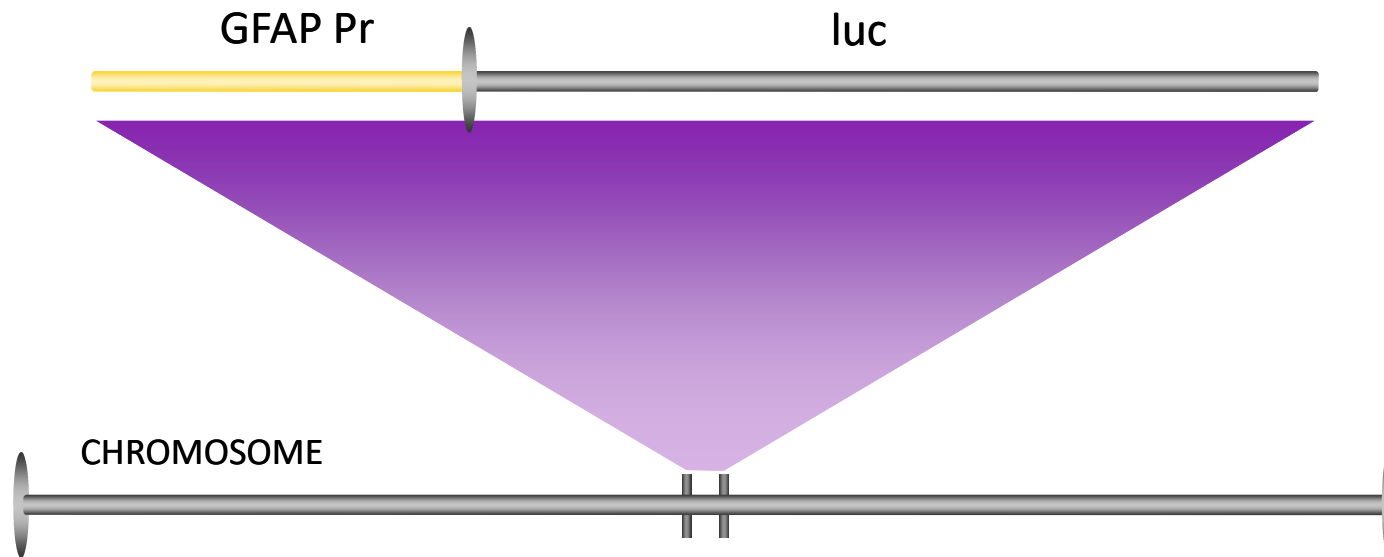
Xenografts of mCherry–SK-Mel-147 cells, imaged in Vegfr3<sup>Luc</sup> reporter mice for wholebody analysis.

Metastatic relapses were found at later time points (involving skin, lymph node and lung metastases) and were **invariably** preceded by V3-Luc emission.

Proteomic analyses identify midkine (MDK) as new prolymphangiogenic and pro-metastatic factor.

The heparin-binding factor **midkine** is a systemic inducer of neo-lymphangiogenesis that defines **patient prognosis**.

## Transgenic Animals: Glial Fibrillary Acidic Protein - Luc



Intermediate Filament Protein Expressed in Astrocytes  
of the CNS Induced by Neuronal Brain Injury

## GFAP as a marker for prion disease

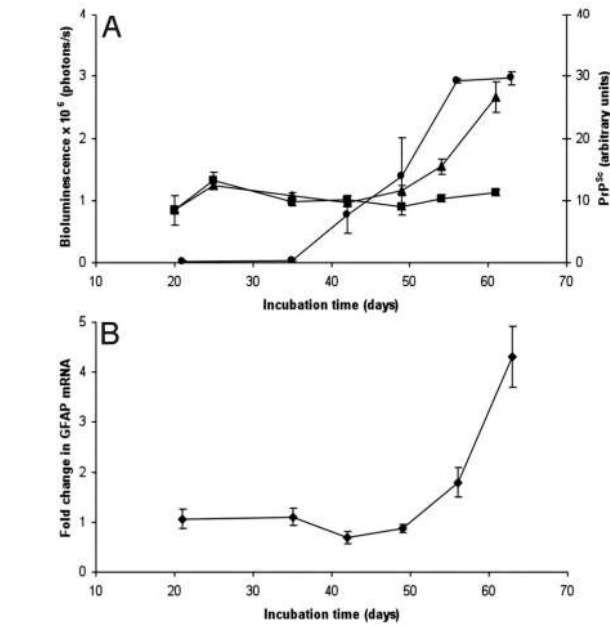
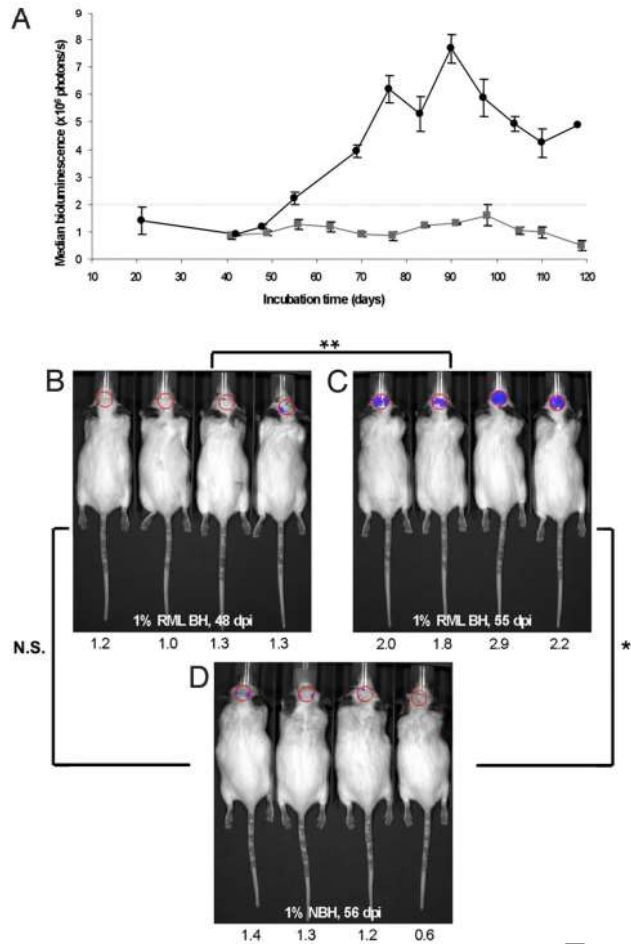


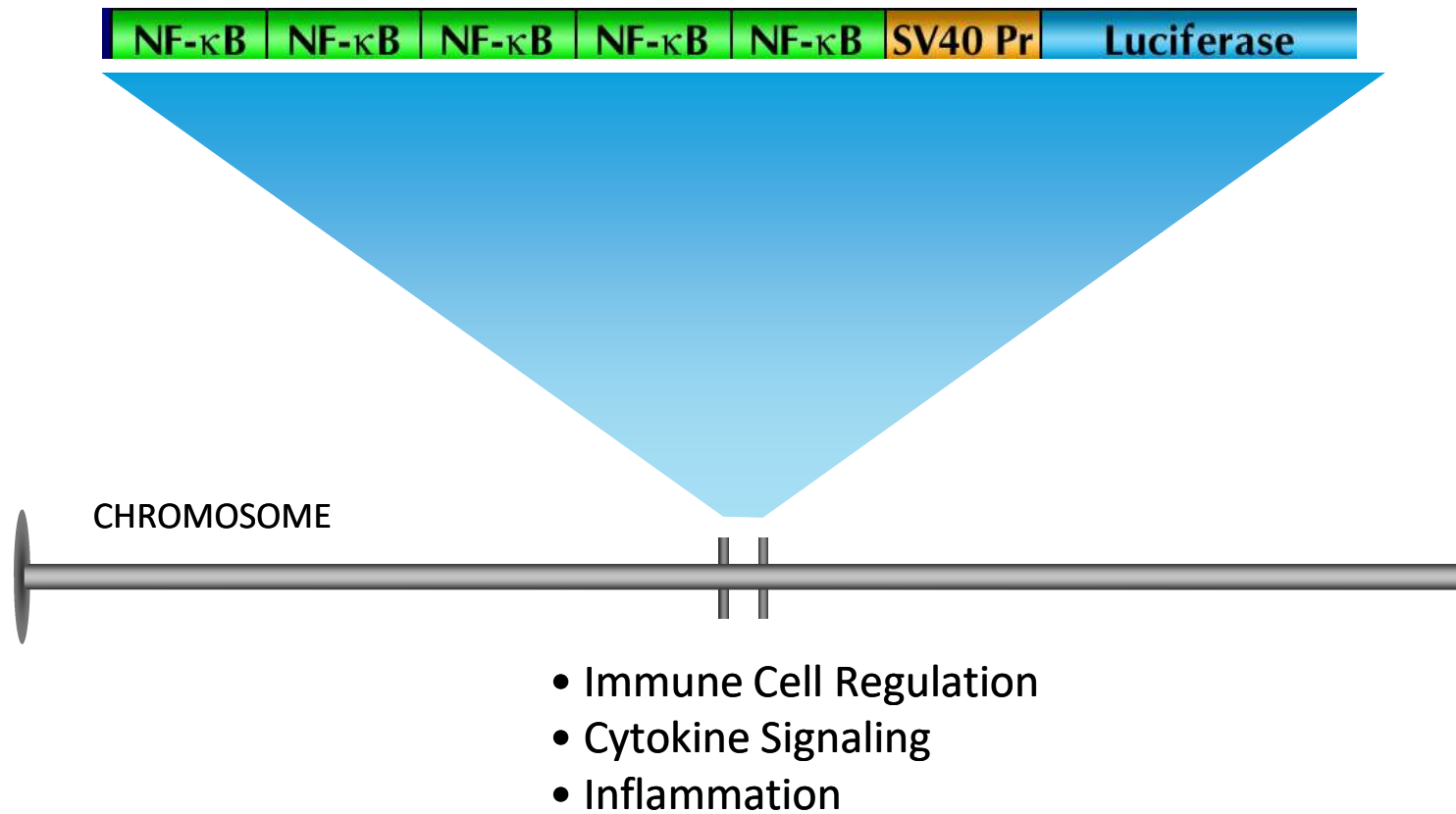
**Fig. 2.** During prion infection, increases in PrP<sup>Sc</sup> preceded increases in BL (A) and GFAP mRNA (B). (A) Protease-resistant PrP<sup>Sc</sup> (circles, right ordinate) in the brains of RML-infected Tg(Gfap-luc) mice began to accumulate at 42 dpi and increased steadily. PrP<sup>Sc</sup> levels were quantified at each time point by densitometry of Western blottings. BL (triangles, left ordinate) in the brains of infected Tg(Gfap-luc) mice increased beginning at 56 dpi, ~14 d after PrP<sup>Sc</sup> accumulation. BL measured from the brains of control mice inoculated with 1% NBH did not increase (squares). (B) Correlating with an increase of BL, GFAP mRNA also increased at ~56 dpi. Error bars indicate the SE, based on at least 9 mice for BL measurements and 3 mice for all other measurements.

- Tg(Gfap-luc) mice
- Detection of light 55 days post inoculation
- 62 days before appearance of neurological deficits

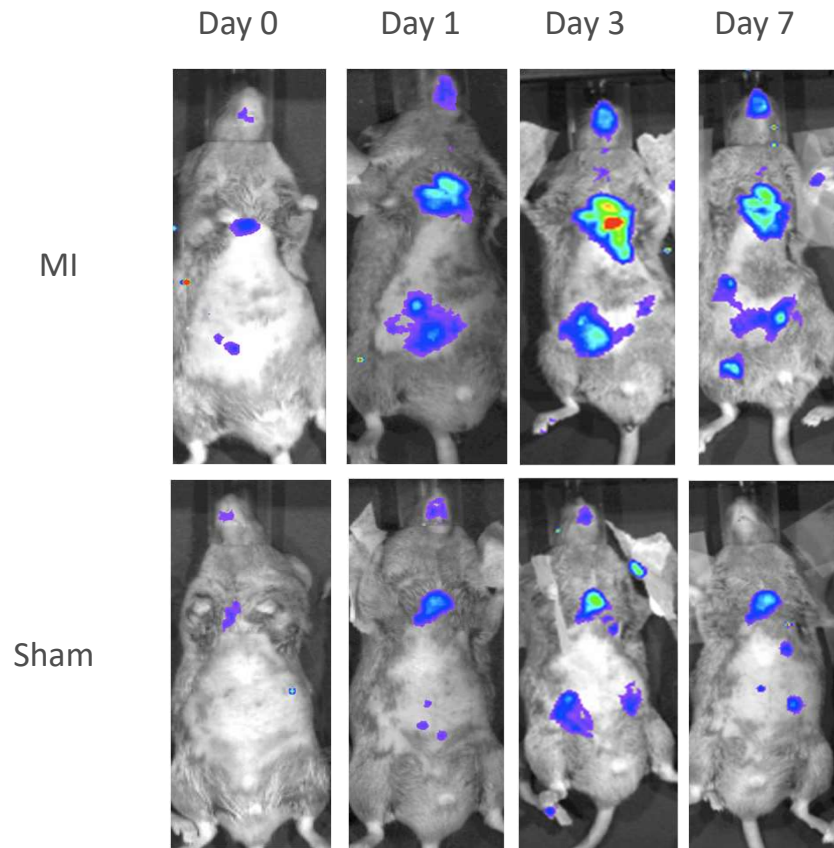
“BLI bioassays were as or more sensitive than those determined by the onset of neurological dysfunction, and were completed in approximately half the time.”

Tamgüney et al., PNAS, 2009

## Transgenic Animals: NF- $\kappa$ B-RE-luc

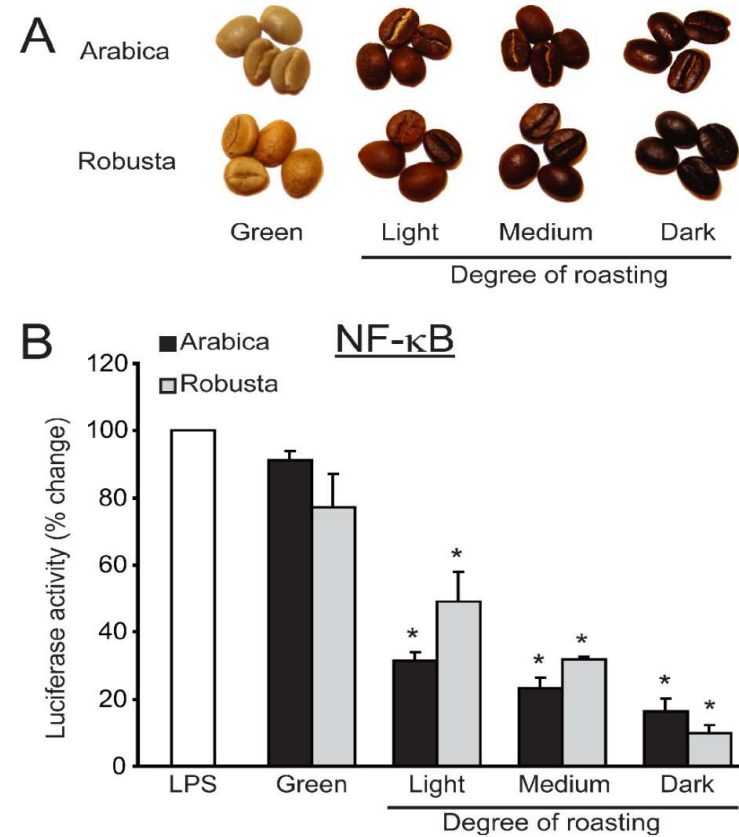
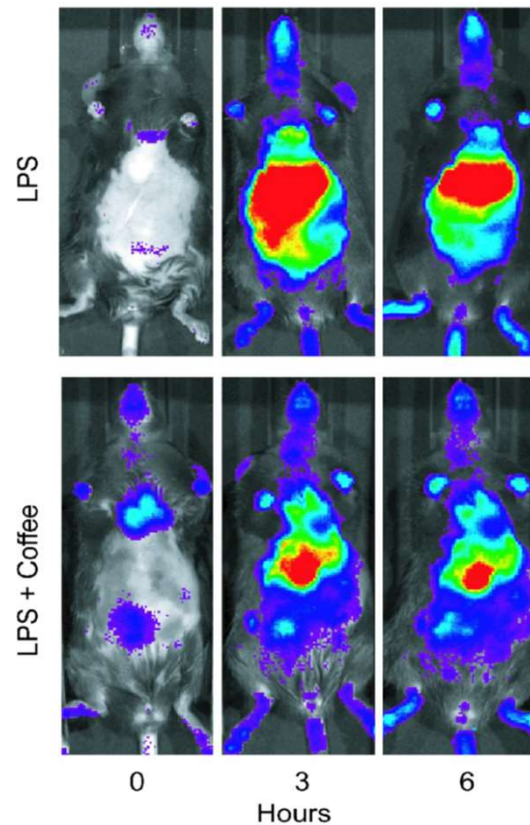


## NF- $\kappa$ B is Increased After Myocardial Infarction



## Effects of Coffee on NF-κB Activity

Transgenic NF-κB reporter mice were given a single dose of coffee extract by oral gavage 3h prior to s.c. LPS injection (at 0h). A) The luciferase activity was measured by *in vivo* imaging at 0h, 3h and 6h





The image features a vibrant yellow background with several large, overlapping, organic shapes that resemble liquid droplets or cells. These shapes have a glossy, reflective quality with highlights and shadows. The word "revvity" is centered in a black, lowercase, sans-serif font. The overall composition is abstract and energetic.

revvity